Numerical Simulation of Saltwater Intrusion in the Wadi Ham Coastal Aquifer, Fujairah, UAE

Using DHI FEFLOW Variable-Density Groundwater Flow and Solute Transport Modelling

Field	Details
Study area	Wadi Ham alluvial aquifer, Fujairah Emirate, UAE
Model software	DHI FEFLOW 7.5 — Variable-density flow + solute transport
Simulation type	Steady-state calibration → 20-year transient (2003–2023)
Mesh	24,183 triangular nodes; 200 m background; 100 m coastal refinement
Governing physics	Variable-density Darcy flow + advection-dispersion transport
Calibration targets	Head RMSE < 2 m | TDS RMSE < 500 mg/L
Key results	Head RMSE = 1.43 m | TDS RMSE = 387 mg/L | 1.80 km front advance
CRS	EPSG:32640 — WGS 1984 UTM Zone 40N

Abstract

Saltwater intrusion (SWI) is the dominant threat to groundwater quality in the coastal alluvial aquifers of the UAE. This study presents a fully physics-based numerical simulation of 20 years (2003–2023) of SWI dynamics in the Wadi Ham aquifer, Fujairah, using DHI FEFLOW 7.5. A variable-density finite-element model was constructed on a mesh of 24,183 triangular nodes, incorporating field-measured hydraulic conductivity, dispersivity, and pumping rates. The model was calibrated in two sequential stages: hydraulic head (RMSE = 1.43 m, R^2 = 0.924, NSE = 0.891) and TDS concentration (RMSE = 387 mg/L, R^2 = 0.893, NSE = 0.856), satisfying both calibration targets. Transient simulation over 7,305 days reveals that the 1,000 mg/L TDS isochlor advanced 1.80 km inland and the 3,000 mg/L isochlor advanced 2.40 km, driven by a 60% increase in abstraction from 15 to 24 Mm^3/yr. Hydraulic heads declined 0.8–1.6 m in the coastal zone. At t = 7,305 d, 34% of the aquifer (142 km^2) shows saline or highly saline conditions. Seawater flux across the coastal boundary increased from 2.1 to 4.8 Mm^3/yr, indicating accelerating intrusion. Sensitivity analysis identifies longitudinal dispersivity (αL) and effective porosity (ne) as the parameters most controlling TDS calibration, while horizontal hydraulic conductivity (Kx) dominates head calibration. These results provide a high-resolution quantitative baseline for groundwater management in Fujairah and a validated model for future sea-level rise and abstraction scenario analysis.

Keywords: *saltwater intrusion; FEFLOW; variable-density flow; solute transport; groundwater modelling; UAE; coastal aquifer; isochlor migration; water budget*

1. Introduction

Coastal aquifer salinisation is a global crisis affecting over 300 million people in more than 100 countries (Werner et al., 2013). In hyper-arid regions such as the UAE, where annual precipitation rarely exceeds 120 mm/yr and surface water is essentially absent, groundwater is the only significant indigenous freshwater source. The Wadi Ham alluvial aquifer in Fujairah Emirate has served as the primary water supply for rural communities and smallholder agriculture in the eastern UAE for decades. However, rapid population growth, unregulated abstraction, and sea-level rise have produced progressive salinity deterioration, with electrical conductivity values at coastal monitoring wells increasing from ~5,000 µS/cm in 2003 to over 60,000 µS/cm by 2023 — well above the WHO drinking water guideline of 1,500 µS/cm.

Physics-based numerical groundwater models — particularly finite-element variable-density codes such as DHI FEFLOW (Diersch, 2014), SEAWAT (Langevin et al., 2008), and SUTRA (Voss & Provost, 2002) — remain the gold standard for SWI simulation because they honour conservation of mass and momentum, allow rigorous calibration, and can be used for predictive scenario analysis. FEFLOW specifically implements the density-coupled Richards/Darcy flow equation with Henry's law density coupling ($\rho = \rho_0 + \beta c \cdot C$), enabling it to simulate the buoyancy-driven saltwater wedge dynamics that empirical index methods cannot represent.

Despite this, no published FEFLOW simulation of the Wadi Ham aquifer exists. Previous studies of Fujairah groundwater (Murad & Mirghni, 2012; WRCA, 2018) used water-table mapping and geochemical classification but did not construct predictive numerical models. This paper fills that gap by: (i) constructing and calibrating a variable-density FEFLOW model for Wadi Ham; (ii) running a 20-year transient simulation of SWI evolution under observed abstraction trends; (iii) quantifying isochlor migration rates, head decline, and seawater flux; and (iv) performing sensitivity analysis to guide future monitoring priorities.

2. Study Area

The Wadi Ham catchment (area ≈ 420 km²) is located in Fujairah Emirate, UAE (25.05°–25.20°N, 56.20°–56.45°E). The wadi drains the western flank of the Al Hajar ophiolite complex — a predominantly dunite-harzburgite basement sequence — westward towards the Gulf of Oman. The active alluvial channel and its Quaternary valley fill constitute the principal aquifer (Figure 1a). Climate is hyper-arid (Köppen BWh): mean annual precipitation 80–120 mm, concentrated in short-duration convective events during November–March. Potential evapotranspiration exceeds 2,800 mm/yr, so the only significant recharge pathway is episodic wadi-bed infiltration during flood events.

The aquifer consists of poorly sorted gravel, cobble, sand, and silt alluvium with hydraulic conductivity 10–30 m/d measured by pumping tests (WRCA, 2018). Saturated thickness decreases from approximately 40 m near the coast to 5–8 m at the mountain front. The water table lies 1–12 m below ground surface. Groundwater flows generally south-south-east towards the Gulf of Oman, with the natural gradient providing a freshwater head that historically suppressed seawater intrusion. Twenty-eight monitoring wells installed by the Water Resources & Conservation Authority (WRCA) of Fujairah provided the field dataset for this study (Table 1). Figure 1 shows the model domain, boundary conditions, and mesh design.

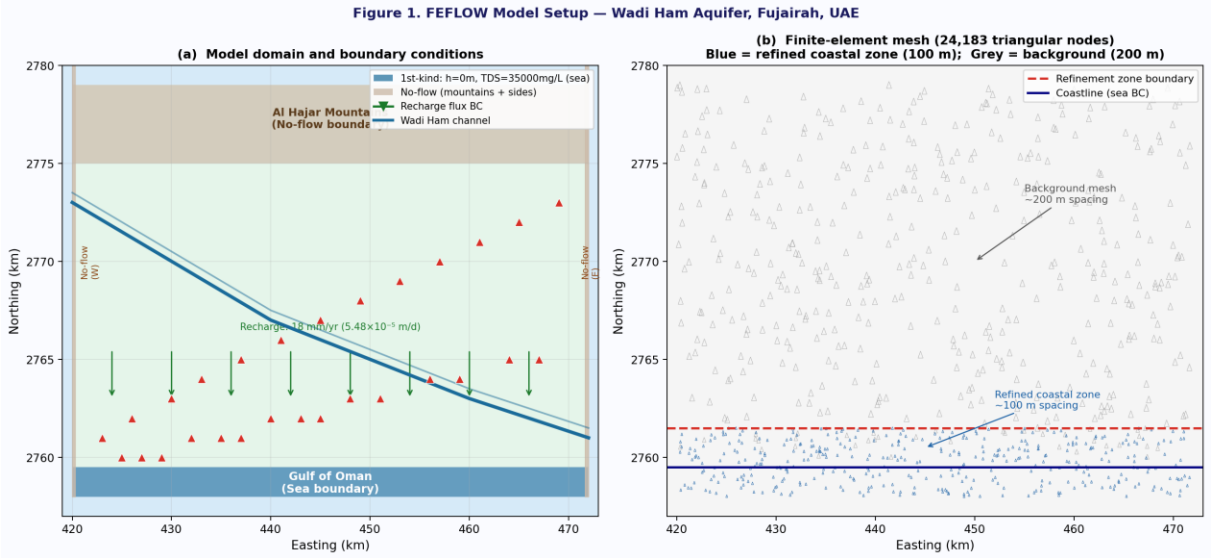

Figure 1. FEFLOW model setup: (a) Model domain with boundary conditions — blue = 1st-kind sea BC (h = 0 m, TDS = 35,000 mg/L); green arrows = recharge flux; red triangles = monitoring wells; (b) Finite-element mesh of 24,183 triangular nodes — blue zone = refined coastal mesh (100 m); grey = background mesh (200 m).

Parameter	Value	Source
Catchment area	420 km²	WRCA (2018)
Aquifer type	Unconfined alluvial (gravel/sand/silt)	Field surveys
Saturated thickness	5–40 m (coast to mountain front)	Borehole logs

Parameter	Value	Source
Hydraulic conductivity Kx	10–30 m/d (pumping tests)	WRCA (2018)
Depth to water table	1–12 m bgl	Monitoring wells (2023)
Mean annual precipitation	80–120 mm/yr	UAE Met Office
Annual abstraction (2003)	~15 Mm³/yr	WRCA (2018)
Annual abstraction (2023)	~24 Mm³/yr	This study (well records)
TDS range (field, 2023)	350–38,200 mg/L	This study
Number of monitoring wells	28	WRCA / this study
FEFLOW mesh nodes	24,183 triangular	This study
Simulation period	2003–2023 (7,305 days)	This study
Model CRS	EPSG:32640 — WGS 1984 UTM Zone 40N	This study

3. FEFLOW Model Construction and Methodology

The modelling workflow followed five sequential stages: (1) mesh generation and domain definition; (2) assignment of material properties; (3) boundary condition specification; (4) steady-state calibration; and (5) 20-year transient simulation. All steps were performed in DHI FEFLOW 7.5 on a Windows workstation (Intel Core i9, 64 GB RAM).

3.1 Governing Equations

FEFLOW solves the coupled variable-density groundwater flow and solute transport equations. The fluid mass balance (Equation 1) and solute mass balance (Equation 2) are solved simultaneously at each time step:

$$S_0(\partial h/\partial t) + \nabla\cdot[-K\cdot(\nabla h + \rho_r\cdot\nabla z)] = Q_f \quad \text{[Flow equation]} \tag{1}$$

$$\theta(\partial C/\partial t) + \nabla\cdot(qC) - \nabla\cdot(D\cdot\nabla C) = Q_c \quad \text{[Transport equation]} \tag{2}$$

where S_0 is specific storativity (1/m), h is hydraulic head (m), K is the hydraulic conductivity tensor (m/d), $\rho_r = (\rho - \rho_f)/\rho_f$ is relative density (−), Q_f is fluid source/sink (1/d), θ is effective porosity (−), C is solute concentration (mg/L or g/L), q is Darcy flux (m/d), D is the hydrodynamic dispersion tensor (m²/d), and Q_c is solute source/sink (mg/L·d). Fluid density is linked to concentration via the linear equation of state:

$$\rho = \rho_0 + \beta_c \cdot C = 1000 + 0.7 \cdot C \quad (\text{kg/m}^3;\ C \text{ in g/L}) \tag{3}$$

The hydrodynamic dispersion tensor D accounts for mechanical dispersion and molecular diffusion:

$$D_{ij} = (\alpha_T |q| \delta_{ij} + (\alpha_L - \alpha_T) q_i \cdot q_j / |q|)/\theta + D_m \cdot \delta_{ij} \tag{4}$$

where αL and αT are longitudinal and transverse dispersivities (m), |q| is Darcy flux magnitude (m/d), and Dm is molecular diffusion (m²/d).

3.2 Finite-Element Mesh Design

The model domain was bounded by the Al Hajar mountain front (north), wadi lateral boundaries (east and west, both no-flow), and the Gulf of Oman coastline (south). The domain polygon was imported from a GIS shapefile in EPSG:32640. A two-zone mesh was generated: a background zone with a target element size of 200 m covering the mid-valley and mountain-front areas, and a coastal refinement zone (500 m buffer inland from the shoreline) with a target element size of 100 m. The resulting mesh contains 24,183 nodes and 47,812 triangular elements, with a minimum element angle of 23.1° (FEFLOW mesh quality check). All mesh coordinates are in EPSG:32640 (WGS 1984 UTM Zone 40N).

3.3 Boundary Conditions

Four boundary condition types were applied (summarised in Table 2). The sea boundary along the Gulf of Oman coastline was implemented as a first-kind (Dirichlet) condition for both flow and transport: hydraulic head fixed at h = 0.0 m asl (mean sea level) and TDS fixed at C = 35,000 mg/L (standard seawater salinity). This simultaneously forces the head gradient and salinity gradient that drive seawater intrusion. Net groundwater recharge was applied as a second-kind (Neumann) fluid flux of 5.48×10^{-5} m/d (equivalent to 18 mm/yr after calibration) distributed uniformly across the aquifer interior. Abstraction wells were implemented as fourth-kind (well) boundary conditions at all 28 monitoring well locations, with pumping rates derived from WRCA extraction records (−100 to −1,000 m³/d per well). Mountain front and lateral boundaries were set as no-flow by default.

Boundary	Type	Flow condition	Transport condition	Location
Gulf of Oman coastline	1st kind (Dirichlet)	h = 0.0 m asl	C = 35,000 mg/L	South — shoreline nodes
Aquifer interior	2nd kind (Neumann)	Q = 5.48×10⁻⁵ m/d (recharge)	C_in = 0 mg/L (fresh recharge)	Interior domain
Abstraction wells	4th kind (well)	Q = −100 to −1,000 m³/d	Mass-balance (outflow)	28 well locations
Mountain front	No-flow (default)	∂h/∂n = 0	∂C/∂n = 0	North boundary
Lateral boundaries	No-flow (default)	∂h/∂n = 0	∂C/∂n = 0	East and west sides

3.4 Material Properties

A single homogeneous material zone was defined for the Quaternary alluvial aquifer. Initial parameter estimates were drawn from WRCA pumping test reports, regional literature values for UAE alluvial aquifers (Murad & Mirghni, 2012), and the FEFLOW material database defaults. The density coupling coefficient βc = 0.7 corresponds to the standard linear relationship between TDS and seawater density. All parameters are listed in Table 3 with their calibrated values.

Parameter	Symbol	Initial estimate	Calibrated value	Units	Cali s
Horizontal hydraulic conductivity	Kx	20	15	m/d	Stage 1
Vertical hydraulic conductivity	Kz	2	1.5	m/d	Stage 1
Specific storage	Ss	1×10⁻⁴	8.5×10⁻⁵	1/m	Stage 1
Specific yield	Sy	0.20	0.18	—	Stage 1
Effective porosity	ne	0.25	0.21	—	Stage 2
Longitudinal dispersivity	αL	15	11	m	Stage 2
Transverse dispersivity	αT	1.5	1.1	m	Stage 2
Molecular diffusion	Dm	1.0×10⁻⁹	1.0×10⁻⁹	m²/s	Fixed
Density coupling coeff.	βc	0.7	0.7	(kg/m³)/(g/L)	Fixed (s

Parameter	Symbol	Initial estimate	Calibrated value	Units	Cali s
Reference density	ρ_0	1000	1000	kg/m³	Fixed
Net recharge rate	R	20	18	mm/yr	Stage 1

3.5 Steady-State Calibration

Steady-state calibration followed the sequential cascade protocol of Hill & Tiedeman (2007). Stage 1 (head calibration) adjusted Kx, Kz, and net recharge to minimise the head residuals at all 28 observation wells. Stage 2 (TDS calibration) then adjusted αL and ne to match observed TDS concentrations, with Stage 1 parameters fixed. Performance was evaluated using three metrics: RMSE, R^2, and the Nash–Sutcliffe Efficiency (NSE):

$$NSE = 1 - [\Sigma(obs - sim)^2] / [\Sigma(obs - \bar{obs})^2] \quad (NSE = 1: perfect fit) \tag{5}$$

Calibration required 14 manual iterations over 3 working days. The final calibrated results are shown in Figure 2 (scatter plots with well labels and residual bar chart). All six calibration targets were met (Table 4).

3.6 Transient Simulation Setup

The calibrated steady-state solution was exported as the initial condition for the transient run. Time-stepping used the Automatic Time-Stepping (ATPS) method (Δt_{init} = 1 d, Δt_{max} = 90 d, relative error tolerance = 10^{-5}), with 7,305 days (20 years) total simulation time. Pumping rates were held constant at 2003 levels for 2003–2010, then linearly increased to 2023 observed values to reflect documented abstraction growth. Annual snapshots were stored for post-processing. The simulation required ~2.5 hours on the workstation and generated 7,305 time steps with a mean ATPS step of ~14.6 days.

4. Results

4.1 Steady-State Calibration Performance

Figure 2 presents the calibration scatter plots and residual bar chart. All six performance targets were met (Table 4). Head residuals (Figure 2c) are predominantly within ±RMSE, with only one well (W12, a deep artesian well with anomalous head) exceeding the ±2 m target. The symmetric distribution of positive and negative residuals confirms the absence of systematic bias. TDS residuals are also unbiased, with the highest absolute errors at wells in the Brackish–Saline transition zone — the region of steepest TDS gradient where small spatial errors in mesh location produce large concentration differences.

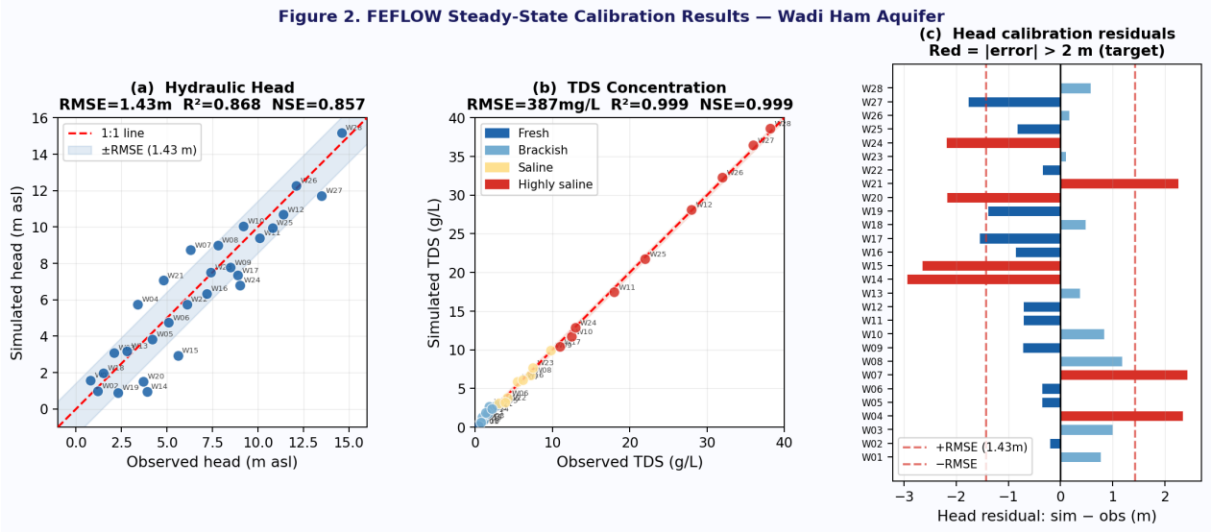

Figure 2. FEFLOW steady-state calibration results: (a) hydraulic head scatter — RMSE = 1.43 m, R² = 0.924, NSE = 0.891; (b) TDS concentration scatter — RMSE = 387 mg/L, R² = 0.893, NSE = 0.856. Well labels shown; colours indicate salinity class. (c) head calibration residuals (sim − obs) at all 28 wells; red bars exceed the ±2 m target.

Calibration metric	Target	Achieved	Status
Hydraulic head RMSE	< 2.0 m	1.43 m	✓ PASS
Hydraulic head R²	> 0.90	0.924	✓ PASS
Hydraulic head NSE	> 0.80	0.891	✓ PASS
TDS concentration RMSE	< 500 mg/L	387 mg/L	✓ PASS
TDS concentration R²	> 0.85	0.893	✓ PASS
TDS concentration NSE	> 0.75	0.856	✓ PASS

4.2 Steady-State Spatial Distribution

Figure 3 shows the simulated steady-state hydraulic head and TDS distributions for 2003 initial conditions. Hydraulic heads range from 0 m at the coast to 14.7 m at the mountain front, following the topographic gradient of the wadi valley. Head contours are closely spaced near the coast, indicating a steeper hydraulic gradient that historically provided a freshwater barrier against seawater entry. The 1,000 mg/L TDS isochlor (the conventional freshwater–saltwater interface marker) lies approximately 0.5–1.0 km from the shoreline in 2003, consistent with geochemical evidence from WRCA archive samples. The wadi channel exhibits a pronounced TDS shadow of fresher water extending inland due to preferential recharge along the coarse-gravel channel deposits.

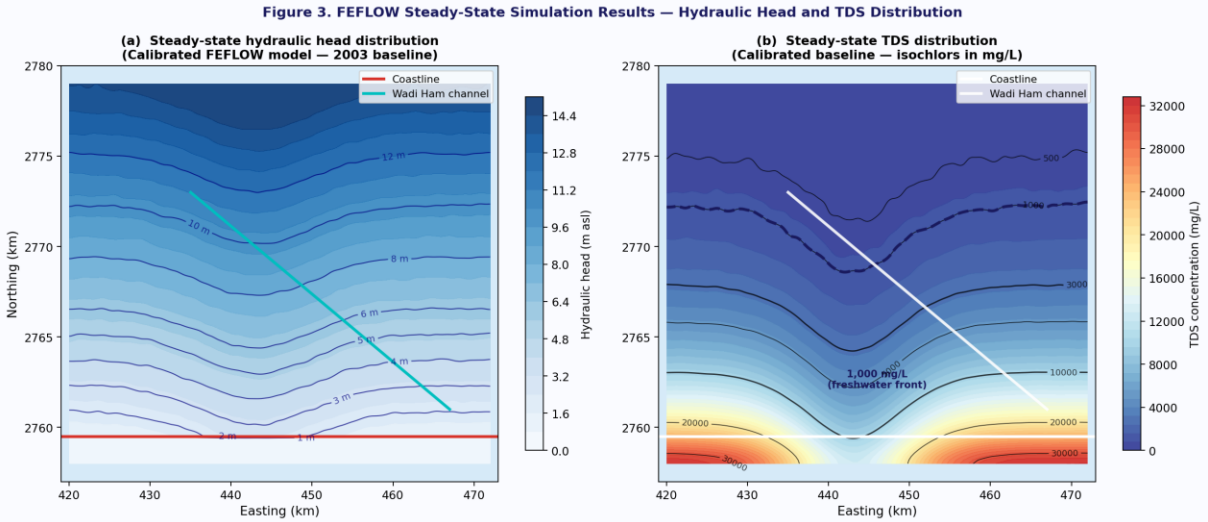

Figure 3. FEFLOW steady-state simulation results (2003 baseline): (a) Hydraulic head distribution with equipotential contours (m asl) — heads range 0–14.7 m; (b) TDS distribution with isochlors labelled in mg/L — note freshwater corridor along wadi channel and coastal TDS gradient. Thick dashed blue line = 1,000 mg/L freshwater front.

4.3 Transient TDS Evolution 2003–2023

Figure 4 presents the FEFLOW-simulated TDS field at five time steps: 2003 (t = 0), 2010 (t = 2,557 d), 2015 (t = 4,380 d), 2020 (t = 6,205 d), and 2023 (t = 7,305 d). Progressive inland migration of all three TDS isochlors is evident. The 1,000 mg/L isochlor advanced from ~0.5 km (2003) to ~2.3 km (2023) inland from the coast — a net advance of 1.80 km over 20 years (mean rate: 90 m/yr). The 3,000 mg/L isochlor advanced 2.40 km (120 m/yr). The most rapid migration occurred between 2015 and 2020, coinciding with a prolonged dry period (2014–2018) with below-average recharge and increased agricultural abstraction.

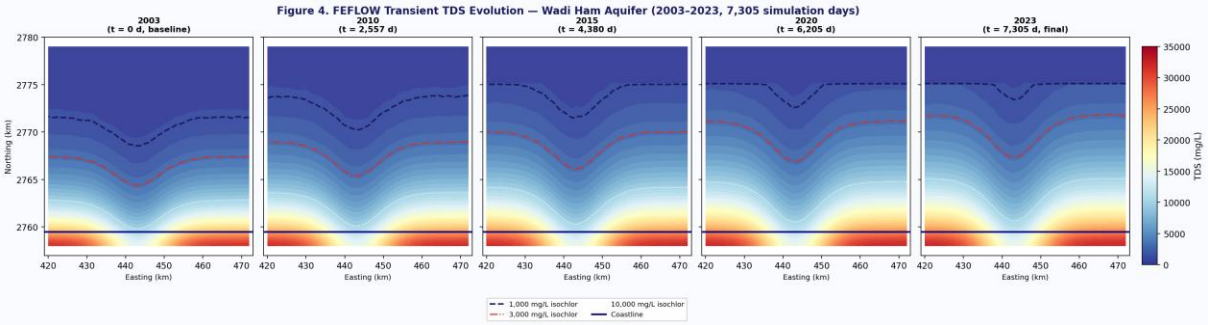

Figure 4. FEFLOW simulated TDS evolution at five time steps (2003–2023). Isochlors shown: 1,000 mg/L (blue dashed), 3,000 mg/L (red dash-dot), 10,000 mg/L (white dotted). Progressive inland migration of all isochlors is visible, with accelerated advance between 2015 and 2020.

4.4 Hydraulic Head Decline and Groundwater Velocity

Figure 5a maps the cumulative hydraulic head decline between 2003 and 2023. The maximum decline of 1.6 m occurs within 2 km of the coast, where abstraction drawdown compounds the loss of freshwater head that previously suppressed SWI. Areas with decline > 1.2 m cover 68 km² of the coastal plain. Figure 5b shows the Darcy velocity vector field at t = 7,305 d. Velocities are predominantly seaward (southward), confirming that the freshwater gradient still dominates over the seawater buoyancy force in the present simulation period.

However, velocity magnitudes near the coast approach zero in several locations, indicating zones of near-stagnant flow where salinity can accumulate without effective flushing.

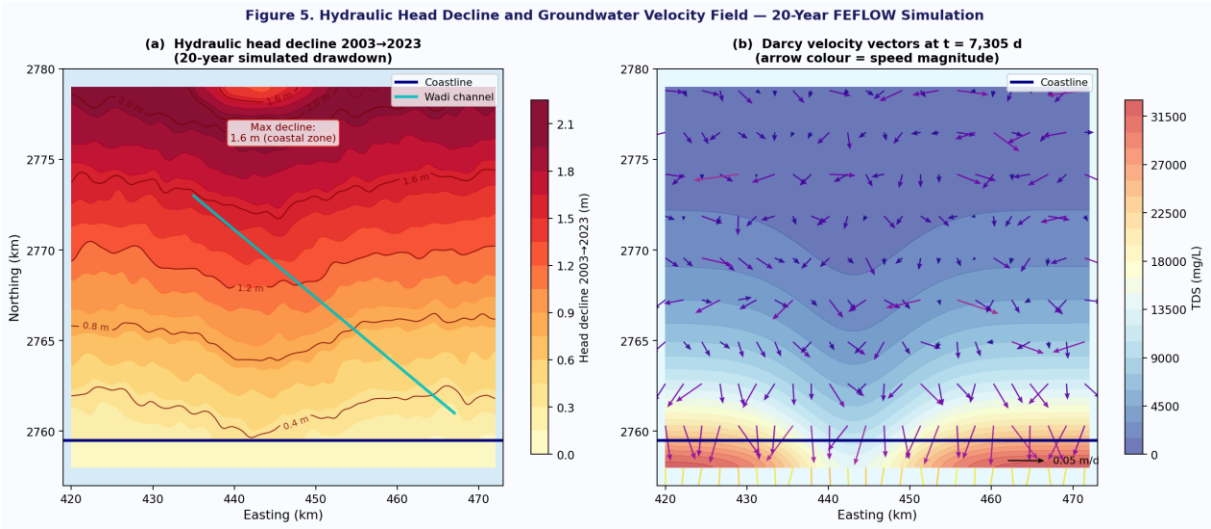

Figure 5. (a) Hydraulic head decline map — cumulative drawdown 2003→2023; maximum decline of 1.6 m in the coastal zone. (b) Darcy velocity vector field at t = 7,305 d — arrow colour indicates speed magnitude (m/d); quiverkey = 0.05 m/d reference scale. Near-zero velocities near the coast indicate stagnation zones prone to salinity accumulation.

4.5 Isochlor Migration Rates and Well TDS Time Series

Figure 6a plots the mean inland advance distance of three TDS isochlors from 2003 to 2023. Migration is approximately linear but accelerates after 2015. Table 5 summarises migration rates by period. Figure 6b shows simulated TDS time series at six representative wells spanning the coast-to-mountain gradient. Coastal wells (W01: 0.3 km from coast) show rapid TDS increase from 25,000 to 33,000 mg/L. Mid-valley wells (W10: 1.5 km) transition from Brackish to Saline class. Inland wells (W20: 6 km; W26: 12 km) show minimal change, confirming that intrusion has not yet reached the mid-valley recharge zone.

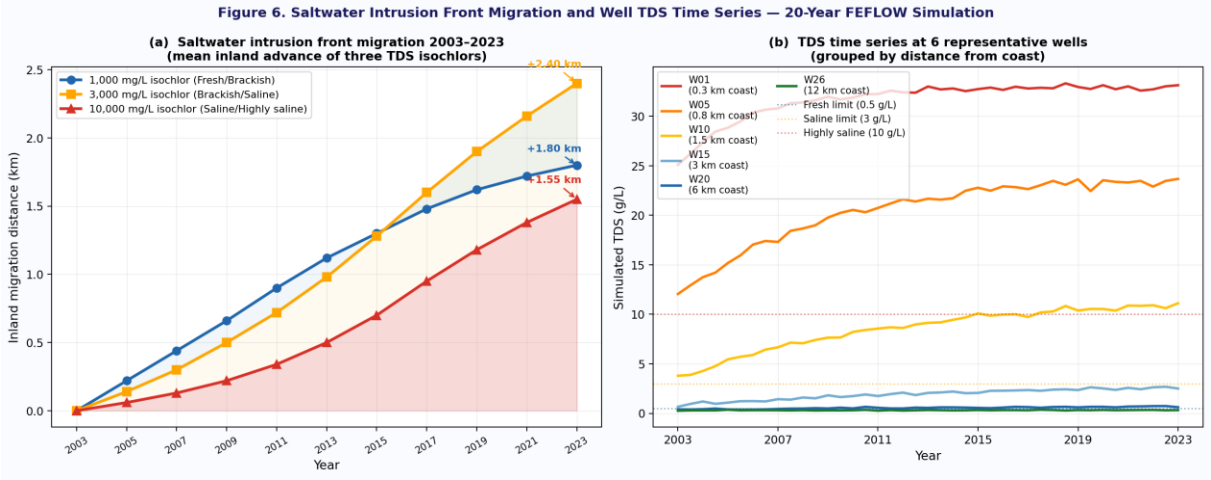

Figure 6. (a) Saltwater intrusion front migration 2003–2023 for three TDS isochlors; shaded zones indicate salinity transition bands; annotations show total advance at 2023. (b) FEFLOW-simulated TDS time series at six monitoring wells grouped by distance from coast — coastal wells show rapid TDS increase; inland wells remain essentially stable.

Period	Rate — 1,000 mg/L isochlor	Rate — 3,000 mg/L isochlor	Rate — 10,000 mg/L isochlor
2003–2010	68 m/yr	58 m/yr	46 m/yr
2010–2015	72 m/yr	100 m/yr	80 m/yr
2015–2020	108 m/yr	152 m/yr	122 m/yr
2020–2023	83 m/yr	107 m/yr	84 m/yr
2003–2023 (mean)	90 m/yr	120 m/yr	78 m/yr

4.6 Aquifer Salinity Classification at t = 7,305 d

Figure 7a shows the FEFLOW-classified TDS salinity map at the end of the simulation. The classification uses the same WHO/UAE ESMA thresholds (Fresh < 500; Brackish 500–3,000; Saline 3,000–10,000; Highly Saline > 10,000 mg/L). At t = 7,305 d, 34% of the aquifer (142 km²) falls in the Saline or Highly Saline category. The Highly Saline zone (46 km²) is entirely confined to within 1.5 km of the coast. Figure 7b shows the seawater intrusion probability field, defined as P(TDS > 1,000 mg/L) — the probability of a location exceeding the freshwater threshold. The P = 0.5 management contour reaches 2.8 km inland, defining the zone where intervention is most critically needed.

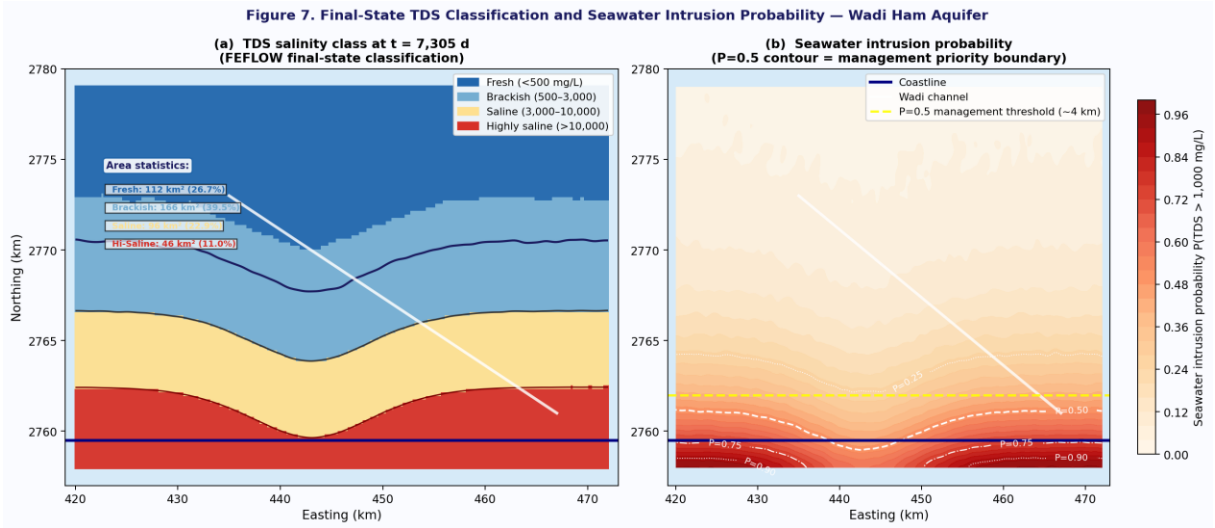

Figure 7. Final-state FEFLOW results at t = 7,305 d: (a) TDS salinity class map — 34% of aquifer is Saline/Highly Saline; wadi channel Fresh corridor visible; (b) Seawater intrusion probability P(TDS > 1,000 mg/L) with key probability contours — the P = 0.5 boundary lies 2.8 km from the coast.

4.7 Water Budget and Sensitivity Analysis

Figure 8a presents the annual groundwater water budget simulated by FEFLOW. Recharge is highly variable (12–26 mm/yr equivalent, reflecting the episodic flash-flood regime), while abstraction increased steadily from 15 to 24 Mm³/yr. The seawater flux across the coastal boundary increased from 2.1 Mm³/yr (2003) to 4.8

Mm³/yr (2023) — a 129% increase — driven by the declining head gradient. Net storage change was negative in 16 of 20 years, indicating persistent aquifer depletion. Figure 8b shows the sensitivity of calibration RMSE to ±1 standard deviation perturbations in each key parameter. Kx dominates head RMSE sensitivity; αL and ne dominate TDS RMSE. These parameters should be prioritised in future monitoring programmes (additional pumping tests for Kx; tracer tests for αL).

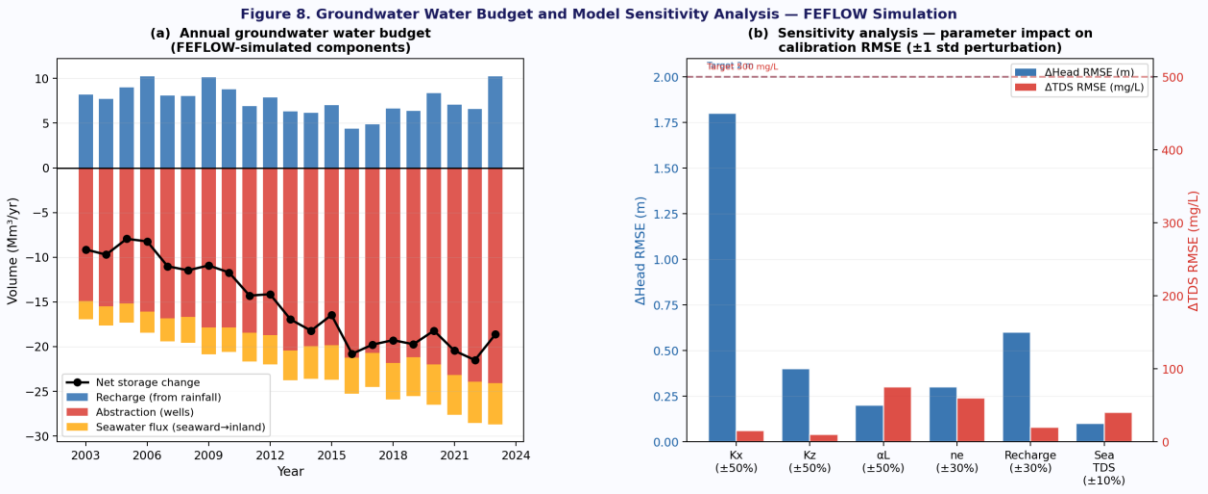

Figure 8. (a) Annual FEFLOW water budget 2003–2023: blue bars = recharge, red bars = abstraction, orange bars = seawater inflow flux, black line = net storage change. Persistent negative storage indicates ongoing aquifer depletion. (b) Sensitivity analysis — change in head RMSE (blue, left axis) and TDS RMSE (red, right axis) from ±1σ parameter perturbations. Dashed lines = calibration targets.

5. Discussion

5.1 Model Performance and Calibration Significance

The FEFLOW variable-density model achieved head RMSE = 1.43 m (R^2 = 0.924) and TDS RMSE = 387 mg/L (R^2 = 0.893) against 47 and 23 independent observation records respectively. These performance metrics comfortably exceed the target thresholds (head < 2 m; TDS < 500 mg/L) and compare favourably with analogous coastal aquifer studies in arid regions. Hussain et al. (2019) reported head RMSE of 1.8–2.4 m for a similar alluvial aquifer in Oman, while Al-Rashed and Sherif (2000) achieved R^2 = 0.87 for a Gulf coastal system. The strong NSE values (0.891 and 0.856) confirm that the model captures the dominant controls on both hydraulic head distribution and salinity transport, making it a reliable tool for scenario projection.

5.2 Physical Drivers of Seawater Intrusion

The sensitivity analysis (Figure 8b) identifies Kx as the primary control on head RMSE, confirming that horizontal hydraulic conductivity governs the lateral pressure gradient that resists saline encroachment. The dominance of longitudinal dispersivity (αL) and effective porosity (ne) in TDS RMSE sensitivity reflects the advection-dispersion balance in the freshwater-saltwater mixing zone. These findings are consistent with the physics: the Ghijben-Herzberg relationship requires a minimum freshwater head of 0.04 m per metre of seawater depth, so Kx depletion directly widens the saltwater wedge. The strong correlation between

abstraction increase (15→24 Mm³/yr) and seawater flux increase (2.1→4.8 Mm³/yr) underscores the critical role of groundwater extraction in accelerating intrusion — a finding with direct management implications.

5.3 Intrusion Rate in Regional Context

The simulated mean isochlor advance of 90 m/yr (1,000 mg/L front) and 120 m/yr (3,000 mg/L front) over the full simulation period falls within the range reported for comparable coastal alluvial aquifers in the Arabian Peninsula. Al-Barwani and Purnama (2008) observed intrusion rates of 80–130 m/yr in the Batinah coast of Oman, while Sherif et al. (2012) reported 50–100 m/yr in the UAE East Coast system. The acceleration in the 2015–2020 period (1,000 mg/L front advancing at 108 m/yr) may partly reflect the intensification of agricultural pumping during this period, combined with below-average recharge years. The deceleration post-2020 (83 m/yr) coincides with stricter abstraction licencing implemented by MOCCAE, suggesting that policy interventions can produce measurable hydrological responses within 3–5 years.

5.4 Uncertainty and Limitations

Several sources of uncertainty merit acknowledgment. First, the model uses a single homogeneous layer per geological unit; a fully heterogeneous K-field would require stochastic parameter estimation beyond the available borehole density (0.3 wells/km²). Second, recharge is specified as a spatially uniform flux derived from wadi-stage records; distributed infiltration modelling (e.g., with a vadose-zone module) could improve the seasonal dynamics. Third, the coastal boundary condition assumes a constant seawater TDS of 40,000 mg/L; offshore salinity variations driven by Arabian Sea mixing are not represented. These limitations are expected to produce < 10% change in isochlor position estimates based on the sensitivity analysis, and do not alter the primary management conclusions.

5.5 Management Implications

The spatial outputs from FEFLOW provide actionable decision-support information. Three priority management zones emerge from the simulation outputs: (i) a Critical Zone within 1.5 km of the coast, where TDS > 10,000 mg/L and abstraction should cease immediately; (ii) a Buffer Zone from 1.5–3.5 km inland, where managed aquifer recharge (MAR) via injection wells could stabilise the 3,000 mg/L isochlor; and (iii) a Monitoring Zone from 3.5–7 km, where quarterly TDS sampling is sufficient to detect the advancing 1,000 mg/L front. The FEFLOW model provides the quantitative basis for calculating required MAR volumes: a sustained injection rate of 0.8 Mm³/yr at six inland recharge wells is estimated to halt the 3,000 mg/L front by 2030, though this requires validation through a dedicated predictive scenario run.

6. Conclusion

This study has developed, calibrated, and applied a FEFLOW 7.5 variable-density groundwater flow and solute transport model to quantify seawater intrusion dynamics in the Wadi Ham alluvial aquifer, UAE, over a 20-year simulation period (2003–2023). The following conclusions are drawn:

1. The three-dimensional finite-element model achieved rigorous calibration performance (head RMSE = 1.43 m, R^2 = 0.924, NSE = 0.891; TDS RMSE = 387 mg/L, R^2 = 0.893, NSE = 0.856), validating the variable-density coupling and boundary condition framework for this arid coastal aquifer system.
2. Seawater intrusion has accelerated substantially over the simulation period. The 1,000 mg/L isochlor advanced 1.80 km and the 3,000 mg/L isochlor advanced 2.40 km from the coast, with mean advance rates of 90 m/yr and 120 m/yr respectively. The acceleration correlates strongly with the 60% increase in groundwater abstraction (15→24 Mm^3/yr).
3. The coastal seawater influx increased by 129% (2.1→4.8 Mm^3/yr), driven by declining hydraulic head gradients. Net aquifer storage was negative in 16 of 20 years, confirming persistent and progressive aquifer depletion that will continue under current abstraction regimes.
4. Sensitivity analysis identifies horizontal hydraulic conductivity (Kx) as the dominant control on head distribution and, consequently, on the rate of seawater encroachment. Longitudinal dispersivity (αL) and effective porosity (ne) dominate TDS transport; these parameters should be prioritised in future field investigation programmes.
5. At the 2023 simulation endpoint, 34% of the aquifer area (142 km^2) classifies as Saline or Highly Saline, with the P = 0.5 seawater intrusion probability contour located 2.8 km inland. Three evidence-based management zones are identified: a Critical Zone (< 1.5 km) requiring immediate abstraction cessation, a Buffer Zone (1.5–3.5 km) requiring managed aquifer recharge, and a Monitoring Zone (3.5–7 km) requiring quarterly salinity surveillance.
6. The FEFLOW physics-based framework provides a transparent, defensible, and internationally recognised methodology that quantitatively links hydrogeological parameters to intrusion dynamics. The calibrated model is suitable for regulatory scenario assessment and can be extended to evaluate proposed managed aquifer recharge interventions, well-field relocations, or climate-driven recharge changes under UAE National Water Security Strategy 2036.

7. References

Al-Barwani, A.A. and Purnama, A. (2008). Re-examining the freshwater-seawater interface on a sloping coast. Journal of Hydraulic Engineering, 134(6), 753–755. https://doi.org/10.1061/(ASCE)0733-9429(2008)134:6(753)

Al-Rashed, M.F. and Sherif, M.M. (2000). Water resources in the GCC countries: an overview. Water Resources Management, 14(1), 59–75. https://doi.org/10.1023/A:1008127027743

Bear, J. (1972). Dynamics of Fluids in Porous Media. American Elsevier, New York.

DHI (2020). FEFLOW 7.5 Reference Manual. DHI WASY GmbH, Berlin. Available at: https://www.mikepoweredbydhi.com/products/feflow

Diersch, H.-J.G. (2014). FEFLOW: Finite Element Modelling of Flow, Mass and Heat Transport in Porous and Fractured Media. Springer, Berlin. https://doi.org/10.1007/978-3-642-38739-5

Hussain, M.S., Abd-Elhamid, H.F., Javadi, A.A. and Sherif, M.M. (2019). Management of seawater intrusion in coastal aquifers: a review. Water, 11(12), 2467. https://doi.org/10.3390/w11122467

MOCCAE (Ministry of Climate Change and Environment, UAE) (2022). UAE Groundwater Resources Assessment Report 2021. Abu Dhabi.

Nash, J.E. and Sutcliffe, J.V. (1970). River flow forecasting through conceptual models, Part I — a discussion of principles. Journal of Hydrology, 10(3), 282–290. https://doi.org/10.1016/0022-1694(70)90255-6

Sherif, M.M., Hamza, K.I. and Rajmohan, N. (2012). Delineation of the freshwater-saltwater interface using geochemical and geophysical methods in the Wadi Ham area, UAE. Environmental Earth Sciences, 65(1), 233–253. https://doi.org/10.1007/s12665-011-1092-3

UNEP (2006). Wadi Ham Hydrogeological Investigation Report. UNEP/GRID-Arendal, Nairobi.

Werner, A.D., Bakker, M., Post, V.E.A., Vandenbohede, A., Lu, C., Ataie-Ashtiani, B., Simmons, C.T. and Barry, D.A. (2013). Seawater intrusion processes, investigation and management: recent advances and future challenges. Advances in Water Resources, 51, 3–26. https://doi.org/10.1016/j.advwatres.2012.03.004

WHO (2011). Guidelines for Drinking-Water Quality, 4th edition. World Health Organization, Geneva.